

Article

Modeling of Novel Thermodynamic Cycles to Produce Power and Cooling Simultaneously

Wilfrido Rivera ^{1,*}, Karen Sánchez-Sánchez ¹, J. Alejandro Hernández-Magallanes ²,
J. Camilo Jiménez-García ³  and Alejandro Pacheco ¹

¹ Instituto de Energías Renovables, Universidad Nacional Autónoma de México, Temixco 62580, Morelos, Mexico; sasak@ier.unam.mx (K.S.-S.); parea@ier.unam.mx (A.P.)

² Facultad de Ciencias Químicas, Universidad Autónoma de Nuevo León, Av. Universidad s/n, Ciudad Universitaria, San Nicolás de los Garza, Nuevo León 66455, Mexico; jahem@ier.unam.mx

³ Area de Ingeniería en Recursos Energéticos, Departamento de Ingeniería de Procesos e Hidráulica, Universidad Autónoma Metropolitana, Campus Iztapalapa, Av. San Rafael Atlixco 186 Col. Vicentina, Iztapalapa CDMX 14387, C.P. 09340, Mexico; jcjig@ier.unam.mx

* Correspondence: wrgf@ier.unam.mx; Tel.: +52-5556229740

Received: 7 February 2020; Accepted: 5 March 2020; Published: 9 March 2020



Abstract: Thermodynamic cycles to produce power and cooling simultaneously have been proposed for many years. The Goswami cycle is probably the most known cycle for this purpose; however, its use is still very limited. In the present study, two novel thermodynamic cycles based on the Goswami cycle are presented. The proposed cycles use an additional component to condense a fraction of the working fluid produced in the generator. Three cycles are modeled based on the first and second laws of thermodynamics: Two new cycles and the original Goswami cycle. The results showed that in comparison with the original Goswami cycle, the two proposed models are capable of increasing the cooling effect, but the cycle with flow extraction after the rectifier presented higher irreversibilities decreasing its exergy efficiency. However, the proposed cycle with flow extraction into the turbine was the most efficient, achieving the highest values of the energy utilization factor and the exergy efficiency. It was found that for an intermediate split ratio value of 0.5, the power produced in the turbine with the flow extraction decreased 23% but the cooling power was 6 times higher than that obtained with the Goswami Cycle.

Keywords: absorption cooling cycles; Goswami cycle; simultaneous power and cooling; ammonia-water

1. Introduction

It has been demonstrated that the consumption of conventional energy sources such as oil, natural gas, and coal, contributes to serious environmental problems, like global warming. In this situation, actions like the use of clean energy sources, the reduction of energy consumption, the efficiency improvement of energy systems, or the minimization and reuse of waste heat energy in industrial processes, become significantly relevant. In the last decades, a lot of research and technological development efforts have been carried out to analyze and propose different ways of producing electricity with minimal economic and environmental impact. This research effort has led to increasingly efficient technologies capable of taking advantage of different types of clean energy or industrial waste heat. A strategy usually considered to increase the efficiency of the cycles for the production of electricity is the implementation of cogeneration systems to make possible the simultaneous production of several types of useful energy, typically electricity and heat, or electricity and cooling effect. Some of the most relevant papers related to producing power and cooling simultaneously are presented in the following.

Kalina [1,2] developed a combined cycle for power generation able to recover waste heat. One of the main differences with the existing vapor cycles was the use of ammonia-water. The efficiencies obtained by the original Kalina cycle and its first versions were between 1.35 and 1.9 times higher than those achieved by the Rankine cycle. El-Sayed and Tribus [3,4] extended the available data for the ammonia-water mixtures and presented a comparison of the Rankine cycle and a modified version of the Kalina cycle. Marston [5] developed several computational models to optimize the simplified Kalina cycle and compared his results with those presented by El-Sayed and Tribus [4]. Park and Sonntag [6] developed a preliminary study of the Kalina cycle in connection with a combined power system. The comparison revealed the superiority of the Kalina cycle over the Rankine cycle, having advantages from the point of view of the first and second laws of thermodynamics. Rogdakis and Antonopoulos [7] suggested a new power cycle working with the ammonia-water mixture and its comparison with the Rankine cycle. The new cycle offered good performance, obtaining first law efficiency values up to 20% higher than those of the Rankine cycle. Nag and Gupta [8] simulated and analyzed the effect of several thermal parameters on the performance of the Kalina cycle. The authors found that the concentration mixture at the inlet of the turbine, as well as the separator temperature, have a significant effect on the system performance. Another case of cycles' comparison is reported by Dejfors et al. [9], who contrasted the performance for a couple of configurations of the Rankine and Kalina cycles when they were used for direct-fired cogeneration applications. In one of the configurations considered, the reheater was not used, and the Rankine cycle offered a power generation between 4% and 11% higher than the offered by the Kalina cycle. In the second case, when the reheater was included, the authors found that the Kalina cycle reached the highest power generation. Goswami [10] proposed a modification of the Kalina cycle, improving the efficiency by the simultaneous production of power and cooling effect. This cycle was understood as a combination of the Rankine cycle using ammonia as the working fluid, and an absorption cooling system operated with the ammonia-water mixture. The authors concluded that the cost of the technology associated with using a solar source to supply the heat to drive the combined cycle was not competitive with that of the fossil-fuel-based technologies. Goswami [10] and Xu et al. [11] proposed a new cycle that was capable of producing power as the primary goal and cooling effect. The novelty of this work was that, instead of carrying out the conventional condensation process, as it was usually performed in the Kalina cycle, an absorption-condensation process was used. From the simulations performed, the authors concluded that this cycle could achieve high thermal efficiencies when it utilized a heat source of approximately 400 K. In addition, the authors proposed some options to get a more competitive cost for this type of plant. Lu and Goswami [12] also analyzed the cycle for power and cooling, but this time focusing on the optimization of the cooling effect instead of the power output, as it had been accomplished by Xu et al. [11]. The authors characterized the thermal behavior for the cycle at different refrigeration temperatures and found that, theoretically, temperatures as low as 205 K could be achieved with this cycle. Hasan et al. [13] performed the optimization of the cycle from the perspective of the second law of thermodynamics. The authors found that the maximum irreversibility took place in the absorber, followed by the rectifier and the solution heat exchanger. In a later study, Hasan et al. [14] investigated the exergy destruction in every component of the cycle. The authors found that the exergy efficiency did not necessarily increase with an increment in the heat source temperature, but that this temperature had an important effect on the fraction of power and cooling produced. Tamm and Goswami [15] experimentally demonstrated the feasibility of the Goswami cycle and compared the experimental results with those obtained from the simulation. Their results showed that the generation and absorption processes approached the expected trends. In addition, it was identified that the thermal efficiency of the cycle was reduced by 20.6%, due to the irreversibilities considered; for the same reason, 11.8% less work output and 37.7% less refrigeration capacity was obtained, respectively. Vijayaraghavan and Goswami [16] investigated the use of several organic working fluids with this cycle and compared their performance with the observed by the conventional mixtures. It was found that the thermodynamic efficiencies of the novel mixtures were lower than those obtained with ammonia-water.

Martin and Goswami [17] proposed a new parameter called effective coefficient of performance (COP) to evaluate the effectiveness of the cooling production in the combined power and cooling cycle. It was found that when the authors used this parameter to optimize the rectifier, the effective COP achieved values of 5; however, when the optimized parameter was the work output, the maximum value for this parameter was just 1.1. An approximation to real operating conditions of the Goswami cycle was proposed and analyzed by Vidal et al. [18], who carried out a simulation utilizing the exergy method to assess the cycle performance. The authors performed the simulation considering reversible and irreversible processes to show the effect of the irreversibilities in each component. The exergy efficiency for the cycle in the irreversible cases was 53% and 51% when the input heat was supplied at temperatures of 125 °C and 150 °C, respectively. Zhang and Lior [19] developed a new combined cycle for power and cooling production, combining an ammonia-water Rankine cycle, and an ammonia refrigeration cycle. Both cycles were interconnected by absorption, separation, and heat transfer processes. For a maximum cycle temperature of 450 °C, the energy and exergy efficiencies obtained were 27.7% and 55.7%, respectively. A novel semi-closed combined cycle for the generation of power and cooling was introduced by Boza et al. [20]. The authors used a semi-closed gas turbine called a high-pressure regenerative turbine engine (HPRTE) and an absorption cooling system. The waste heat from the exhaust gas of the HPRTE was utilized to power the absorption cooling system. The authors analyzed the cycle performance for two cases: Work output of 10 kW and 40 kW. A more detailed parametric analysis for the Goswami cycle was performed by Demirkaya et al. [21], who modeled the cycle. The authors demonstrated that when the ammonia vapor was superheated after the rectification process, the cycle efficiencies increased, but the cooling capacities decreased. The dynamic modeling of a novel cooling, heat, power, and water microturbine combined cycle was carried out by Ryu et al. [22]. The proposed cycle was able to offer some benefits, including increased efficiency, high part-power efficiency, low lapse rate, compactness, low emissions, lower air and exhaust flow, and condensation of cold water. Padilla et al. [23] proposed a combined Rankine–Goswami cycle and analyzed its thermodynamic performance. The authors reported that the maximum first and second law effective efficiencies were 36.7% and 24.7%, respectively. Mendoza et al. [24] proposed the use of low-capacity absorption cooling systems to produce power and refrigeration with a scrolled expander and working fluids like ammonia-water, ammonia-lithium nitrate, and ammonia-sodium thiocyanate. The proposed system achieved different capacities of power and cooling. After this investigation, the same group of work extended the analysis of the combined cycles for taking advantage of the mid-temperature heat sources. Ayoub et al. [25] analyzed several combined cycles for the simultaneous or alternative production of power and refrigeration. The authors concluded that an interesting application for the combined cycles was the efficient use of solar thermal installations throughout the year to produce variable amounts of electricity and cooling according to specific building demand, thus reducing the consumption of primary energy significantly. Muye et al. [26] investigated the annual performance of an absorption power and cooling system using solar energy, utilizing the ammonia-water mixture and a biomass auxiliary system. It was concluded that an increase in the heat source temperature benefited the power production but not the cooling power; also, it was demonstrated that an increase in the cooling water temperature resulted in a detriment of both cycle outputs: Power and cooling. Barkhordarian et al. [27] proposed a novel power and cooling cycle operated with the ammonia-water mixture for two cooling temperature levels by using two evaporators. It was found that the cycle achieved an exergy efficiency of 38.97% and a thermal efficiency of 19% for the studied case. An innovative cascading cycle involving an organic Rankine cycle and an adsorption refrigeration cycle was proposed by Jiang et al. [28]. The working fluids utilized in both cycles were refrigerant 245fa and silica-gel/LiCl. The system achieved maximum values for power and cooling of 232 kW and 4.94 kW, respectively, for a driving temperature of 95 °C, a cooling water temperature of about 25 °C, and a chilled water temperature of 10 °C. The exergy efficiencies for the cascading system were better than those of the pumpless ORC and the absorption chiller when the hot water temperature was 95 °C. Shankar and Srinivas [29] and Shankar et al. [30] analyzed a solar cooling

cogeneration plant that consists of a Kalina cycle with extra components such as a dephlegmator, a separator, a superheater, a subcooler, and an extra throttling valve. In the simulation, the energy is supplied by a solar collector and a fuel furnace. The authors compare the performance of the proposed system with an absorption cooling plant and a power plant operating individually under the same operating conditions, and the authors concluded that the proposed system is more efficient than the conventional systems. The highest energy utilization factor reported by the authors was 0.39.

As can be seen from the bibliographic review, there have been several studies related to the Goswami cycle. Most of this research has been focused mainly on three topics: The maximization of the first and second law efficiencies, the search of the optimum operative conditions for incrementing either the power or the cooling capacities, and the analysis of the effect that several important parameters have on the system performance. However, none of the articles presented in the literature reviewed are based on the Goswami cycle adding only a condenser and an expansion valve to significantly increase the cooling effect by taking advantage of the latent heat of vaporization. Neither was any study found that analyzed the operation of the system based on flow extractions in the turbine at an intermediate pressure, or after the regenerator to increase the cooling effect. Therefore, in the present study, two novel cycles capable of producing power and cooling simultaneously are presented. The proposed cycles are analyzed and compared to each other and with the Goswami cycle reported in the literature.

2. System Description

2.1. Goswami Cycle (Model I)

An amount of heat \dot{Q}_G is supplied to the generator to desorb part of the working fluid from the absorbent, but since the ammonia-water mixture is a zeotropic fluid, a small amount of water is evaporated together with the ammonia (7). A rectifier is used to condensate the evaporated water, which returns to the generator (8), producing almost pure ammonia vapor (9). An amount of heat \dot{Q}_R is supplied in the reheater to increase the temperature of the ammonia in the vapor phase. The ammonia leaving the reheater passes to the turbine (10), producing an amount of power \dot{W}_T . The ammonia leaving the turbine at lower pressure and temperature (11) passes to the cooler, producing the cooling effect \dot{Q}_E . The working fluid then passes to the absorber (12), where it is absorbed by the solution with low ammonia concentration coming from the generator, delivering an amount of heat \dot{Q}_A . The solution leaving the absorber (1) is pumped to the economizer (2), where it is heated (3) by the solution leaving the generator (4), which reduces its temperature (5) and then passes through the expansion valve (6) before entering the absorber, starting the cycle again. The indicated numbers correspond to the streamlines in Figure 1.

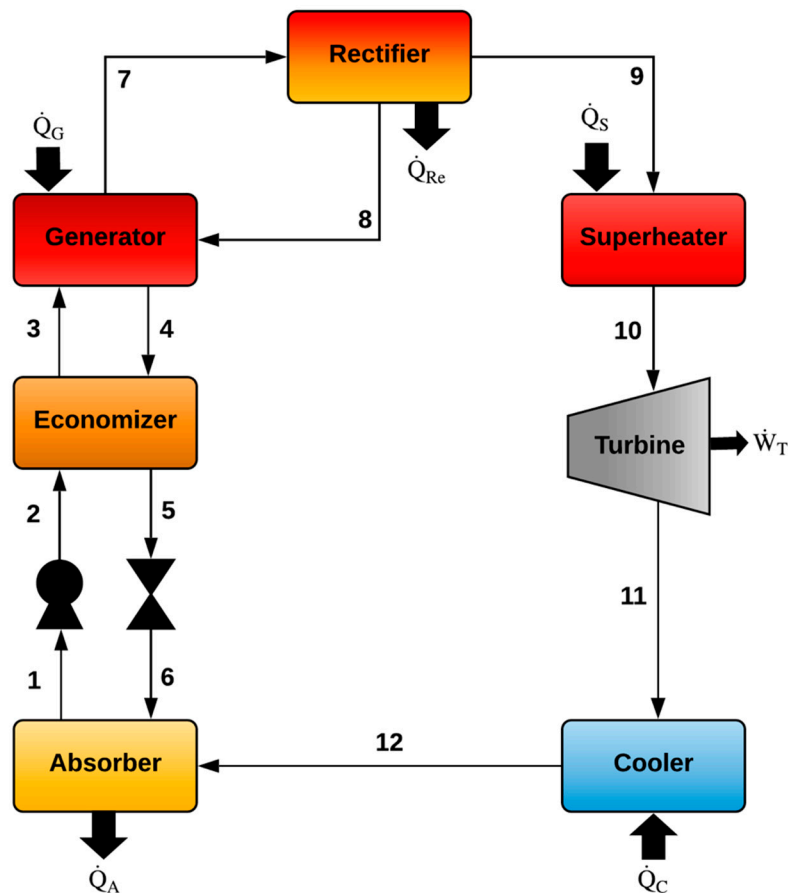


Figure 1. Goswami cycle.

2.2. Goswami Cycle with a Condenser and a Flow Division after the Rectifier (Model II)

This cycle operates in a very similar manner to the Goswami cycle previously described in Section 2.1, but a condenser has been added to condensate part of the ammonia produced in the generator, as can be seen in Figure 2. At the exit of the rectifier (9), the working fluid is split into two streams, one stream goes to the condenser (14) where it is condensed (15) and then expanded through the expansion valve reducing its pressure and temperature (16), while the remaining fluid continues to the reheater (13), and then to the turbine (10) to produce power as in the Goswami Cycle. The ammonia leaving the turbine (11), and the condenser enters the evaporator (17), producing the cooling effect. The ammonia in the vapor phase, leaving the evaporator, goes to the absorber (12), where it is absorbed by the solution leaving the generator. The rest of the cycle operates in a similar way to the Goswami cycle described previously. It is important to mention that in the present cycle, the heat exchanger where the cooling effect takes place is named an evaporator, instead of cooler as in the Goswami cycle. This change in the nomenclature occurs since, in the proposed cycle, the cooling effect is mainly produced by the latent heat of the ammonia, which changes from the liquid phase to the vapor phase, while in the Goswami cycle the cooling effect is mainly produced by the sensible heat gained by the vapor of the working fluid.

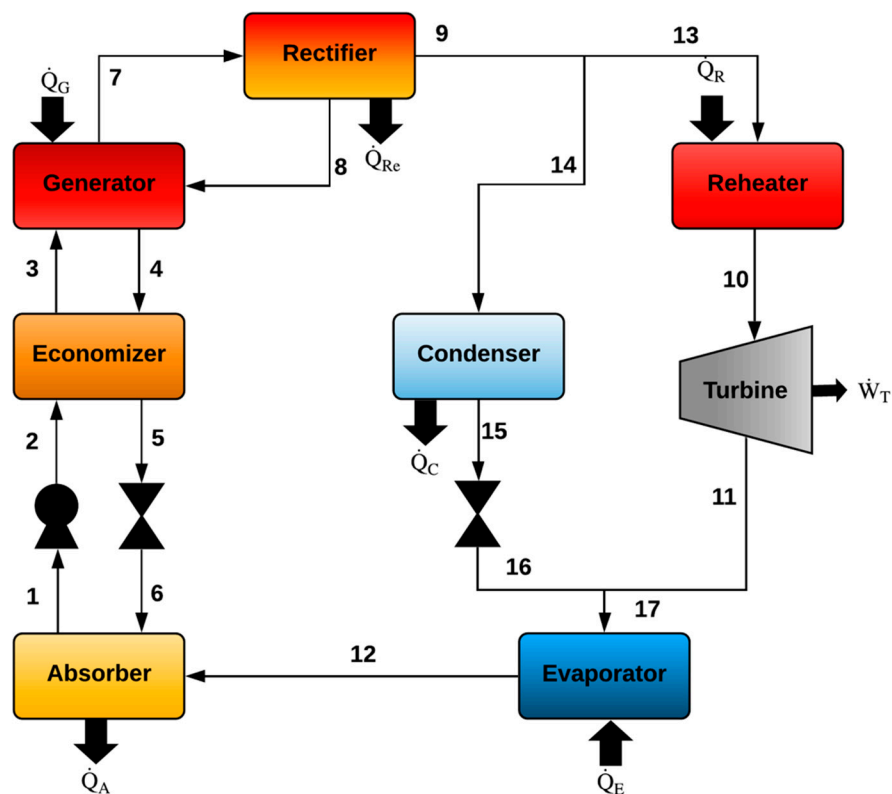


Figure 2. Goswami cycle with a condenser and a flow division after the rectifier.

2.3. Goswami Cycle with a Condenser and a Flow Division into the Turbine (Model III)

This cycle is similar to the modified Goswami cycle, described in Section 2.2, but in the present cycle, a fraction of the ammonia in the vapor phase entering the turbine (10) is extracted at an intermediate pressure (13) to be condensed in the condenser as can be seen in Figure 3. The ammonia in the liquid phase leaving the condenser (14) passes through the expansion valve, reducing its pressure and temperature (15). The rest of the ammonia, which is not extracted, is completely expanded in the turbine producing power. The ammonia leaving the turbine (11) is mixed with the ammonia leaving the condenser before entering the evaporator (16). The total amount of ammonia enters the evaporator producing the cooling effect. The rest of the cycle operates in a similar way to that described by the two previous cycles.

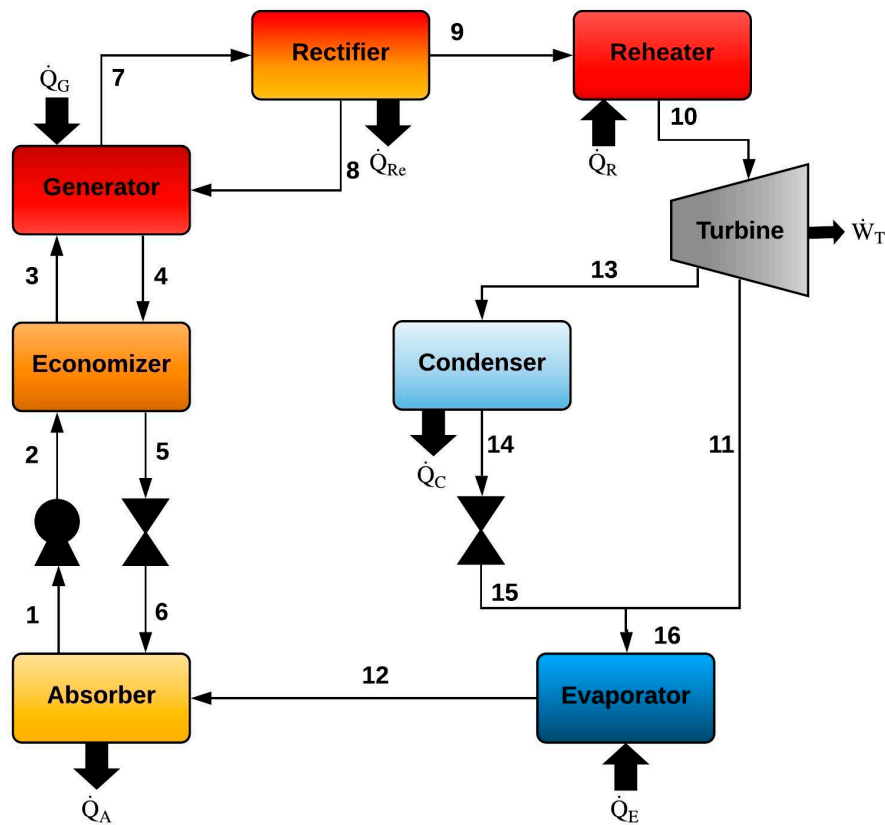


Figure 3. Goswami cycle with a condenser and a flow division into the turbine.

3. Mathematical Model

The mathematical model is based on energy, total mass, and individual species mass balances for each component of the system.

3.1. Assumptions

The following assumptions were considered in the development of the mathematical models for the three cycles:

- Thermodynamic equilibrium conditions are considered in each cycle.
- The cycles operate in steady-state conditions.
- Heat losses from the components are considered negligible.
- The refrigerant is considered in saturation conditions at the exit of the condenser.
- The solution is considered in saturation conditions at the exit of the absorber and generator.
- Pressure losses due to friction are neglected in each component, with the exception of the expansion valves and the turbine.
- The throttling process in the valves is isenthalpic.

3.2. Main Equations

Besides the thermal loads in the heat exchangers, the power produced by the turbine and the work consumed by the pump, the other three important parameters were utilized to evaluate the performance of the system, being these the following:

The energy utilization factor (EUF) is defined as the useful energy produced either in the form of heat or work divided by the energy supplied to the system [31], which can be written as:

$$EUF = \frac{\dot{Q}_E + \dot{W}_{net}}{\dot{Q}_G + \dot{Q}_R} \quad (1)$$

where \dot{Q}_E , \dot{Q}_G , \dot{Q}_R , represent the heat loads in the evaporator, generator, and reheater, respectively, while \dot{W}_{net} represents the net power produced by the cycle calculated as the power produced by the turbine \dot{W}_T minus the power consumed by the pump \dot{W}_P .

Although the EUF is a useful parameter, which indicates the total amount of useful energy produced by a system, this parameter has the problem of adding different types of energy, such as heat and work. For this reason, it is important to use another expression that does not have the mentioned problem, as it is the case of the exergy efficiency, which is defined as the useful exergy produced divided by the exergy consumed by the system, which can be written as:

$$\eta_{EX} = \frac{\dot{W}_{net} + \left(\frac{T_0 - T_E}{T_E}\right)\dot{Q}_E}{\dot{Q}_G\left(1 - \frac{T_0}{T_G}\right) + \dot{Q}_R\left(1 - \frac{T_0}{T_R}\right)} \quad (2)$$

where T_0 represents the environment temperature, and the rest of the variables have the conventional meaning.

The third parameter, related to the exergy efficiency, is the irreversibility, which indicates the exergy lost by the system, and it is calculated as the useful exergy delivered by the system minus the exergy supplied to it.

$$\dot{I} = \left[\dot{Q}_G\left(1 - \frac{T_0}{T_G}\right) + \dot{Q}_R\left(1 - \frac{T_0}{T_R}\right) \right] - \left[\dot{W}_{net} + \dot{Q}_E\left(\frac{T_0 - T_E}{T_E}\right) \right] \quad (3)$$

The main equations used for the simulation of the Goswami cycle (Model I), the Goswami cycle modified with a flow division and using a condenser (Model II) and the Goswami cycle modified with a flow extraction in the turbine and using a condenser are presented in Tables 1–3, respectively.

Table 1. Main equations for the Goswami cycle.

Goswami Cycle (Model I)	
Generator (G)	Absorber (A)
$\dot{m}_3 + \dot{m}_8 = \dot{m}_4 + \dot{m}_7$	$\dot{m}_6 + \dot{m}_{12} = \dot{m}_1$
$\dot{m}_3X_3 + \dot{m}_8X_8 = \dot{m}_4X_4 + \dot{m}_7X_7$	$\dot{m}_6X_6 + \dot{m}_{12}X_{12} = \dot{m}_1X_1$
$\dot{m}_3h_3 + \dot{m}_8h_8 + \dot{Q}_G = \dot{m}_4h_4 + \dot{m}_7h_7$	$\dot{m}_6h_6 + \dot{m}_{12}h_{12} = \dot{m}_1h_1 + \dot{Q}_A$
Rectifier (Re)	Economizer (EC)
$\dot{m}_7 = \dot{m}_8 + \dot{m}_9$	$\dot{m}_2h_2 + \dot{m}_4h_4 = \dot{m}_3h_3 + \dot{m}_5h_5$
$\dot{m}_7X_7 = \dot{m}_8X_8 + \dot{m}_9X_9$	$\eta_{EC} = (h_3 - h_2)/(h_4 - h_2)$
$\dot{m}_7h_7 = \dot{m}_8h_8 + \dot{m}_9h_9 + \dot{Q}_{Re}$	Pump (P)
Reheater (R)	$\dot{W}_P = \dot{m}_1(h_2 - h_1)/\eta_P$
$\dot{m}_9h_9 + \dot{Q}_R = \dot{m}_{10}h_{10}$	$EUF = (\dot{W}_{net} + \dot{Q}_C)/(\dot{Q}_G + \dot{Q}_R)$
Turbine (T)	$\eta_{EX} = \frac{\dot{W}_{net} + \left(\frac{T_0 - T_E}{T_E}\right)\dot{Q}_E}{\dot{Q}_G\left(1 - \frac{T_0}{T_G}\right) + \dot{Q}_R\left(1 - \frac{T_0}{T_R}\right)}$
$\dot{W}_T = \eta_T(\dot{m}_{10}h_{10} - \dot{m}_{11}h_{11})$	$\dot{I} = \left[\dot{Q}_G\left(1 - \frac{T_0}{T_G}\right) + \dot{Q}_R\left(1 - \frac{T_0}{T_R}\right) \right] - \left[\dot{W}_{net} + \dot{Q}_E\left(\frac{T_0 - T_E}{T_E}\right) \right]$
Cooler or Evaporator (C)	
$\dot{m}_{11}h_{11} + \dot{Q}_E = \dot{m}_{12}h_{12}$	

Table 2. Main equations for the Goswami cycle with flow division.

Goswami Cycle with a Condenser and a Flow Division after the Rectifier (Model II)	
Generator (G)	Absorber (A)
$\dot{m}_3 + \dot{m}_8 = \dot{m}_4 + \dot{m}_7$	$\dot{m}_6 + \dot{m}_{12} = \dot{m}_1$
$\dot{m}_3X_3 + \dot{m}_8X_8 = \dot{m}_4X_4 + \dot{m}_7X_7$	$\dot{m}_6X_6 + \dot{m}_{12}X_{12} = \dot{m}_1X_1$
$\dot{m}_3h_3 + \dot{m}_8h_8 + \dot{Q}_G = \dot{m}_4h_4 + \dot{m}_7h_7$	$\dot{m}_6h_6 + \dot{m}_{12}h_{12} = \dot{m}_1h_1 + \dot{Q}_A$
Rectifier (Re)	Economizer (EC)
$\dot{m}_7 = \dot{m}_8 + \dot{m}_9$	$\dot{m}_2h_2 + \dot{m}_4h_4 = \dot{m}_3h_3 + \dot{m}_5h_5$
$\dot{m}_7X_7 = \dot{m}_8X_8 + \dot{m}_9X_9$	$\eta_{EC} = (h_3 - h_2)/(h_4 - h_2)$
$\dot{m}_7h_7 = \dot{m}_8h_8 + \dot{m}_9h_9 + \dot{Q}_{Re}$	Pump (P)
Reheater (R)	$\dot{W}_P = \dot{m}_1(h_2 - h_1)/\eta_P$
$\dot{m}_{13}h_{13} + \dot{Q}_R = \dot{m}_{10}h_{10}$	Condenser (C)
Turbine (T)	$\dot{m}_{14}h_{14} = \dot{m}_{15}h_{15} + \dot{Q}_C$
$\dot{W}_T = \eta_T(\dot{m}_{10}h_{10} - \dot{m}_{11}h_{11})$	$EUF = (\dot{W}_{net} + \dot{Q}_E)/(\dot{Q}_G + \dot{Q}_R)$
Evaporator (E)	$\eta_{EX} = \frac{\dot{W}_{net} + \left(\frac{T_0 - T_E}{T_E}\right)\dot{Q}_E}{\dot{Q}_G\left(1 - \frac{T_0}{T_G}\right) + \dot{Q}_R\left(1 - \frac{T_0}{T_R}\right)}$
$\dot{m}_{17}h_{17} + \dot{Q}_E = \dot{m}_{12}h_{12}$	
$SR = \frac{\dot{m}_{14}}{\dot{m}_9}$	
$\dot{i} = \left[\dot{Q}_G\left(1 - \frac{T_0}{T_G}\right) + \dot{Q}_R\left(1 - \frac{T_0}{T_R}\right)\right] - \left[\dot{W}_{net} + \dot{Q}_E\left(\frac{T_0 - T_E}{T_E}\right)\right]$	

Table 3. Main equations for the Goswami cycle with flow extraction in the turbine.

Goswami Cycle with a Condenser and a Flow Division into the Turbine (Model III)	
Generator (G)	Absorber (A)
$\dot{m}_3 + \dot{m}_8 = \dot{m}_4 + \dot{m}_7$	$\dot{m}_6 + \dot{m}_{12} = \dot{m}_1$
$\dot{m}_3X_3 + \dot{m}_8X_8 = \dot{m}_4X_4 + \dot{m}_7X_7$	$\dot{m}_6X_6 + \dot{m}_{12}X_{12} = \dot{m}_1X_1$
$\dot{m}_3h_3 + \dot{m}_8h_8 + \dot{Q}_G = \dot{m}_4h_4 + \dot{m}_7h_7$	$\dot{m}_6h_6 + \dot{m}_{12}h_{12} = \dot{m}_1h_1 + \dot{Q}_A$
Rectifier (Re)	Economizer (EC)
$\dot{m}_7 = \dot{m}_8 + \dot{m}_9$	$\dot{m}_2h_2 + \dot{m}_4h_4 = \dot{m}_3h_3 + \dot{m}_5h_5$
$\dot{m}_7X_7 = \dot{m}_8X_8 + \dot{m}_9X_9$	$\eta_{EC} = (h_3 - h_2)/(h_4 - h_2)$
$\dot{m}_7h_7 = \dot{m}_8h_8 + \dot{m}_9h_9 + \dot{Q}_{Re}$	Pump (P)
Reheater (R)	$\dot{W}_P = \dot{m}_1(h_2 - h_1)/\eta_P$
$\dot{m}_9h_9 + \dot{Q}_R = \dot{m}_{10}h_{10}$	Condenser (C)
Turbine (T)	$\dot{m}_{13}h_{13} = \dot{m}_{14}h_{14} + \dot{Q}_C$ $PR = P_H/P_{Int}$
$\dot{m}_{10} = \dot{m}_{11} + \dot{m}_{13}$	$EUF = (\dot{W}_{net} + \dot{Q}_E)/(\dot{Q}_G + \dot{Q}_{Re})$
$\dot{W}_T = \eta_T(\dot{m}_{10}h_{10} - \dot{m}_{11}h_{11} - \dot{m}_{13}h_{13})$	$\eta_{EX} = \frac{\dot{W}_{net} + \left(\frac{T_0 - T_E}{T_E}\right)\dot{Q}_E}{\dot{Q}_G\left(1 - \frac{T_0}{T_G}\right) + \dot{Q}_R\left(1 - \frac{T_0}{T_R}\right)}$
Evaporator (E)	
$\dot{m}_{17}h_{17} + \dot{Q}_E = \dot{m}_{12}h_{12}$	
$SR = \frac{\dot{m}_{13}}{\dot{m}_{10}}$	
$\dot{i} = \left[\dot{Q}_G\left(1 - \frac{T_0}{T_G}\right) + \dot{Q}_R\left(1 - \frac{T_0}{T_R}\right)\right] - \left[\dot{W}_T + \dot{Q}_E\left(\frac{T_0 - T_E}{T_E}\right)\right]$	

3.3. Input Data

The input data for the modeling of the three cycles are listed in Table 4. As can be seen, the range of the generation temperature was set at 90 to 150 °C, simulating the waste heat supplied by an industrial process. The rest of the parameters have conventional values.

Table 4. Input data.

Variable	Operation Range	Increment
P_H (kPa)	2000–4000	500
T_E (°C)	−10–10	5
$T_A = T_C$ (°C)	20–40	5
T_G (°C)	90–150	10
ΔT (°C)	10–50	20
SR (-)	0–1	0.1
η_P (-)	0.80	
η_{EC} (-)	0.70	
η_T (-)	0.85	
xR	0.995	
mr (kg/s)	1	

3.4. Algorithm

The algorithm followed for the simulation of the Model III is shown in Figure 4. The algorithms for Model I and II are similar but eliminating all related with the intermediate pressure. The input parameters were: The temperatures of generation ($T_G = T_7$), evaporation, ($T_E = T_{12}$) and absorption ($T_A = T_1$), the temperature difference in the reheater (ΔT), the high pressure (P_H), the Split Ratio (SR), the mass of the refrigerant (mr), the economizer effectiveness (η_{EC}), the pump efficiency (η_P), and the turbine efficiency (η_T). The system was modeled operating with the ammonia-water mixture. The physical properties were taken from Ibrahim and Klein [32]. Appendix A shows all the data obtained from the modeling for the nominal case.

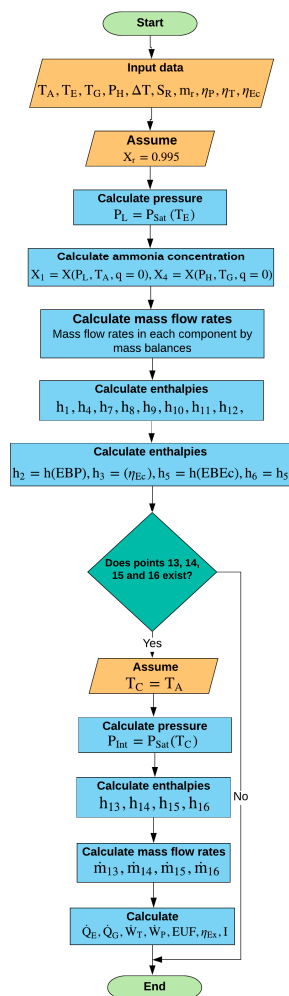


Figure 4. Algorithm flow chart for the modeling of the three cycles.

4. Results

Since the behavior of the Goswami cycle operating with the ammonia-water mixture has been previously reported by other authors [10,12]. This section is structured in the following way. Section 4.1 shows the results of the first cycle proposed (Model II). Section 4.2 shows the behavior of the second system proposed (Model III), and Section 4.3 shows the performance comparison for the two proposed cycles regarding the Goswami cycle.

4.1. Goswami Cycle with a Condenser and a Flow Division after the Rectifier (Model II)

Figures 5–8 illustrate the results of the modeling of the Goswami cycle modified including a flow division at the exit of the generator and the use of a condenser for a case base, which considers a $P_H = 3000$ kPa, a $T_G = 130$ °C, a $T_C = 30$ °C and an increment of temperature in the reheater $\Delta T = 10$ °C.

Figure 5 illustrates the power produced by the turbine and the cooling effect produced in the evaporator as a function of the split ratio (SR) of the working fluid extracted after the rectifier. A value of $SR = 0$ means that all the ammonia in the vapor phase passes to the turbine, while a value of $SR = 1$, means that all the working fluid goes to the condenser. As can be seen from the figure, \dot{W}_T decreases while \dot{Q}_E increases with the increment of SR. For an $SR = 0$, the maximum \dot{W}_T produced by the system is 250 kW with a \dot{Q}_E about 100 kW; however, for an intermediate value of SR, which can be for instance 0.5, although \dot{W}_T decreases to a value of 115 kW (at a $T_E = -10$ °C), \dot{Q}_E increases significantly up to a value of about 600 kW, which is 600% higher than the cooling effect produced at $SR = 0$. This fact can be an advantage for industries that require a significant cooling effect. On the other hand, it can be observed that the evaporator temperature affects \dot{W}_T at low SR values, but the effect is also negligible at higher SR values. In addition, it can be seen that \dot{Q}_E does not have a significant change with the variation of the evaporator temperature.

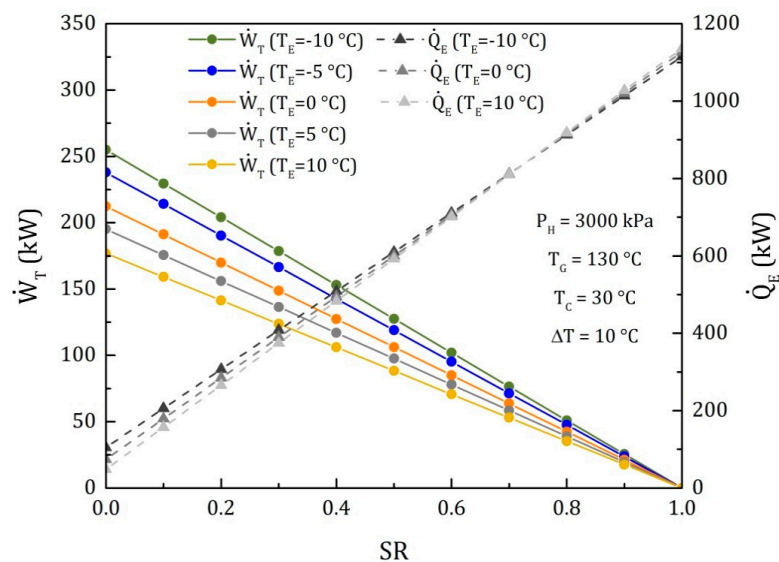


Figure 5. \dot{W}_T and \dot{Q}_E as a function of SR for Model II for different evaporator temperatures.

The variation of the EUF as a function of SR for different evaporator temperatures is illustrated in Figure 6. The EUF values increased with an increment of SR. The minimum values of the EUF were obtained at $SR = 0$, varying between 0.10 and 0.17. The maximum values were achieved at $SR = 1$, varying between 0.32 and 0.79, which were between 3 and 6 times higher than the minimum values. This significant increase was due to the considerable increment of \dot{Q}_E showed in Figure 6, according to Equation (1). In addition, it can be seen that the evaporator temperature considerably affects the EUF for higher values of SR, since when $SR = 1$, the maximum EUF was 0.32 at a $T_E = -10$ °C, while at $T_E = 10$ °C the EUF was 0.79.

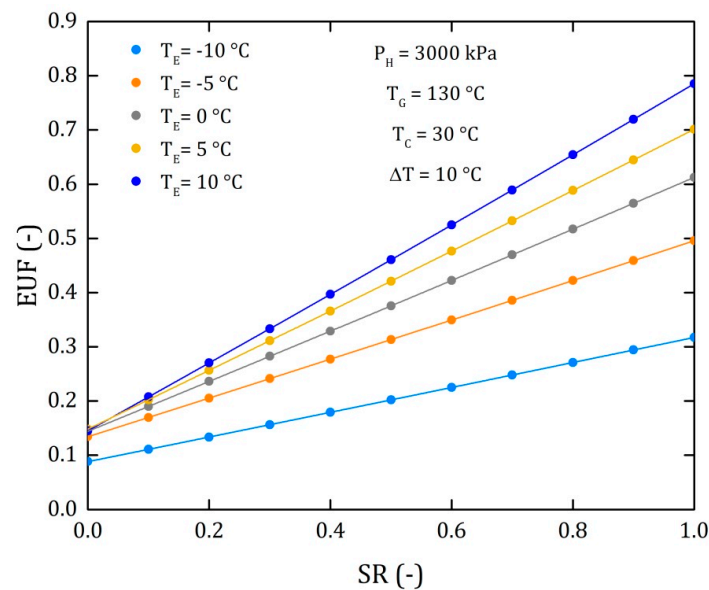


Figure 6. Energy utilization factor (EUF) as a function of split ratio (SR) for Model II for different evaporator temperatures.

As mentioned in Section 3.2, although the EUF is a useful parameter, which indicates the total amount of useful energy produced by a system, this parameter has the problem of adding different types of energy. For this reason, Figure 7 illustrates the exergy efficiency as a function of the evaporator temperature for three different values of SR. At $SR = 0$ the η_{EX} values are the highest since all the ammonia in the vapor phase is supplied to the turbine to produce power, which is high-quality energy, while at $SR = 1$ the η_{EX} values are the lowest since all the ammonia is used as heat, which is low-quality energy. In addition, it can be observed that the η_{EX} values increase and then remain almost constant and even decrease with the increment of the evaporator temperature. This behavior occurred because \dot{Q}_E increases with the increment of T_E ; however, at higher T_E values, the term of temperatures that multiplies \dot{Q}_E in Equation (2) considerably decreases, thus decreasing η_{EX} .

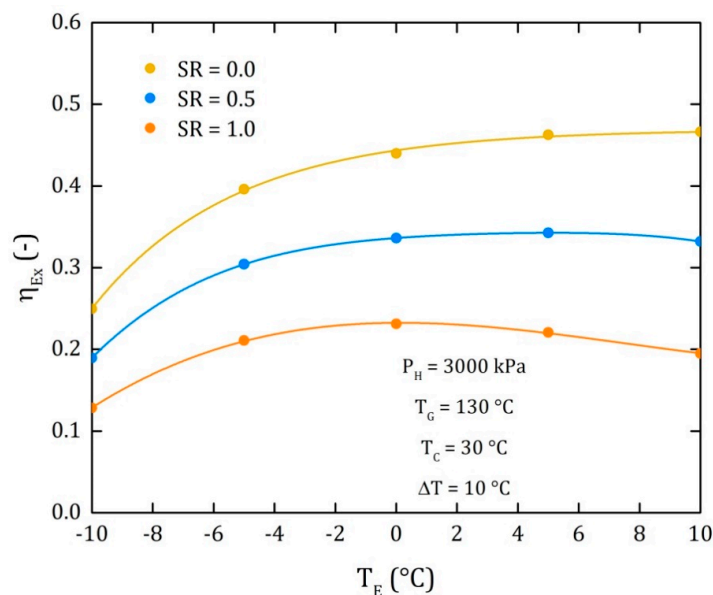


Figure 7. η_{EX} as a function of T_E for Model II at three different values of SR.

Figure 8 illustrates the system's irreversibilities as a function of the evaporator temperature for three different values of SR. The results plotted in this figure are related to the variation of the η_{EX} values reported in Figure 7 since as it can be observed, the irreversibilities decrease with the increment of T_E , which is the opposite to the variation of η_{EX} . This behavior was expected since a decrease in the irreversibilities led to an increase of η_{EX} . In addition, it can be seen that the irreversibilities are the lowest at SR = 0 since in this case, all the ammonia produced was used in the turbine to produce power.

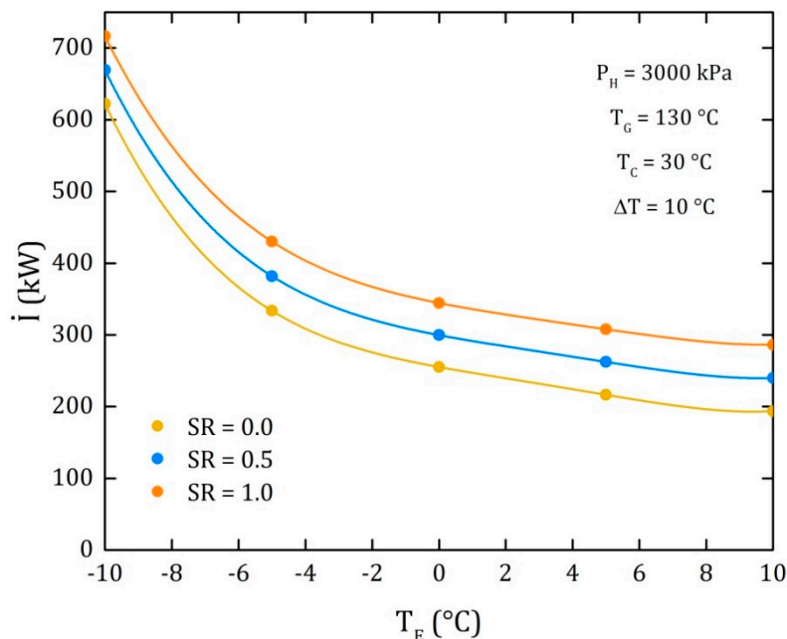


Figure 8. Irreversibility as a function of T_E for Model II at three different values of SR.

From the analysis of this cycle, it can be concluded that the system has the capability of producing higher amounts of cooling power, which can be useful for certain type of industries that require a great amount of cooling and not too much electric power; however, from the exergy point of view, the system is less efficient as the SR values increase.

4.2. Goswami Cycle with a Condenser and a Flow Division into the Turbine (Model III)

Figures 9–12 illustrate the modeling results of the Goswami cycle, including a condenser and a flow division into the turbine, for the same base case set in Section 4.1 for Model II.

Figure 9 illustrates the power produced by the turbine and the cooling effect as a function of SR of the ammonia extracted from the turbine at an intermediate pressure. In the present cycle, a value of SR = 0 means that all the ammonia is expanded throughout the entire turbine, while SR = 1 means that all the ammonia is extracted at an intermediate pressure to go to the condenser. As can be seen in Figure 5, \dot{W}_T decreases while \dot{Q}_E increases with the increment of SR. It was proven that for an SR = 0, the \dot{W}_T values were exactly the same as those reported in Figure 5 since all the ammonia was expanded through the turbine. However, at SR = 1, the \dot{W}_T was not zero, as in Figure 5, since in the present cycle, all the ammonia was expanded in the turbine at an intermediate pressure. For an intermediate value of SR = 0.5, the \dot{W}_T decreased to a value of 170 kW (at a $T_E = -10$ °C), but \dot{Q}_E significantly increased to a value of about 600 kW, which was 6 times higher than the cooling effect produced at SR = 0. As was shown in Figure 5, in Figure 9 it can be observed that the evaporator temperature affects \dot{W}_T at low SR values, but its effect was also negligible at high SR values.

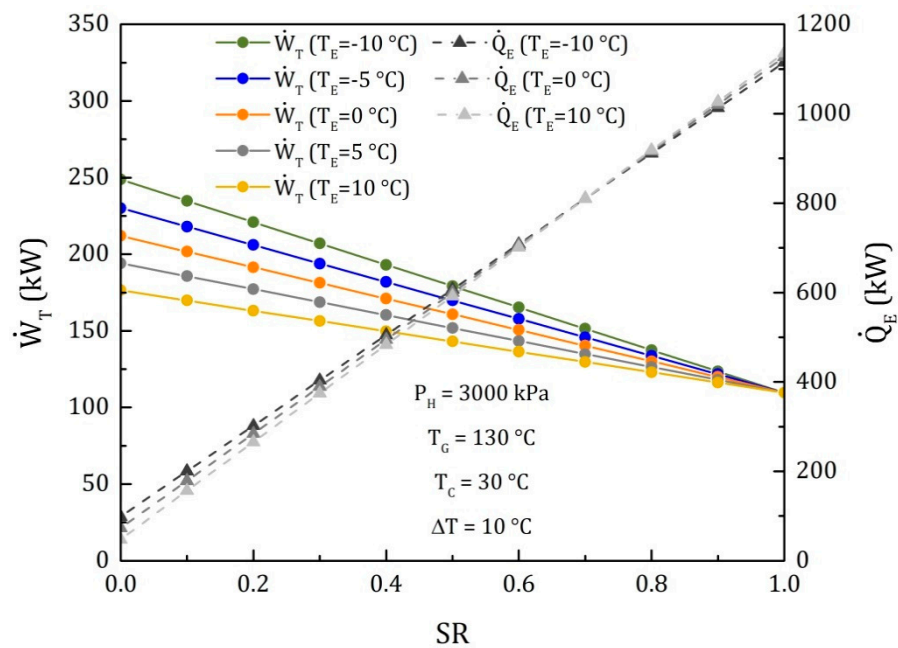


Figure 9. \dot{W}_T and \dot{Q}_E as a function of SR for Model III for different evaporator temperatures.

Figure 10 illustrates the EUF as a function of SR at different evaporator temperatures. In a similar way, as in Figure 6, the EUF values significantly increased with the increment of SR. The minimum values of the EUF were obtained at SR = 0, varying between 0.10 and 0.17, while the maximum values achieved at SR = 1 were in a range between 0.35 and 0.84, being between 3 and 6 times higher than the minimum values. In addition, these values were considerably higher than those achieved by Shankar and Srinivas [30], who reported a maximum energy utilization factor of 0.39 for their proposed cycle. As was mentioned previously, this significant increase was due to the considerable increment of \dot{Q}_E illustrated in Figure 9. In addition, it can be seen that evaporation temperature considerably affects the EUF at higher values of SR.

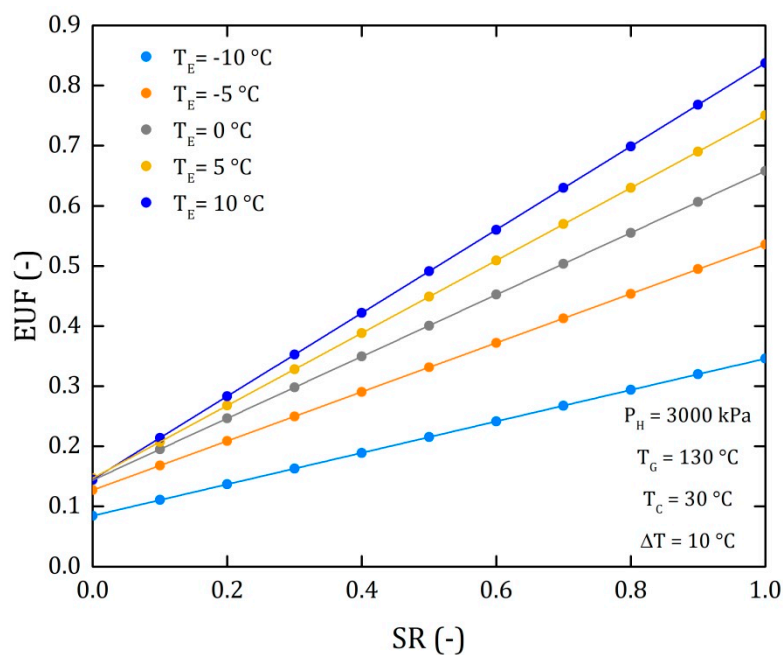


Figure 10. EUF a function of SR for Model III for different evaporator temperatures.

Figure 11 illustrates the η_{EX} as a function of the evaporator temperature at three different values of SR for Model III. As can be observed, the η_{EX} rapidly increases with an increment in the evaporator temperatures and then remains almost constant for the three different SR values. This behavior occurred because the exergy required in the generator to produce a cooling effect at low evaporator temperatures is very high, which reduces η_{EX} . However, as the evaporator temperature increases, the exergy required in the generator decreases following an asymptotic behavior. On the other hand, it can be seen that the η_{EX} values are slightly higher at higher SR values. This behavior is opposite to that illustrated in Figure 7. This effect takes place since, in the present cycle, the energy and exergy are more efficiently used, since the cooling power produced is similar to that obtained with Model II, but the power produced with Model III is considerably higher. The highest value of the exergy efficiency is 50%, which is considerably higher than the value reported by Padilla et al. [23], which was 24%, but lower than that reported by Zhang and Lior [19], which was 55.7%. However, the proposed cycle has the advantage of requiring fewer components than the cycle proposed by Zhang and Lior [19] since their system consists, in fact, of two cycles (the power cycle and the cooling cycle) operating in parallel.

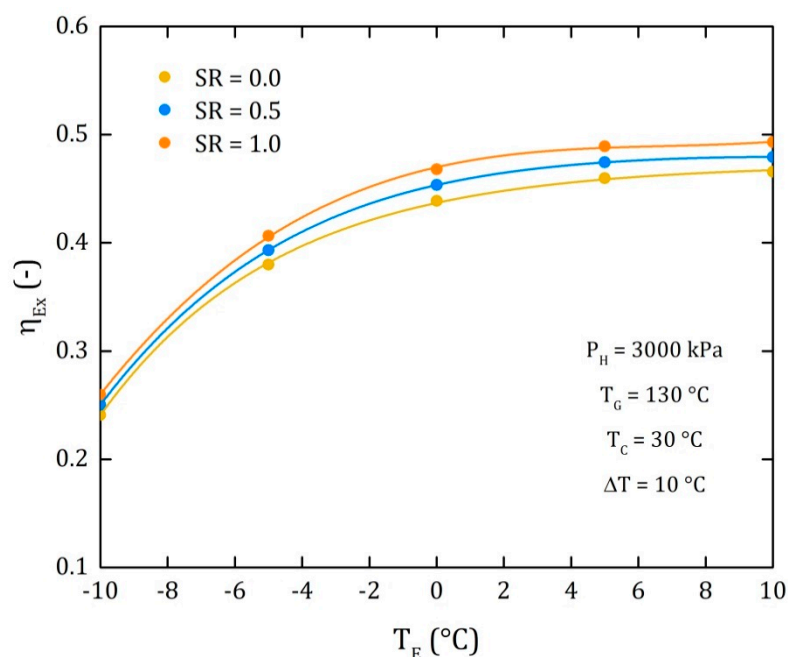


Figure 11. η_{EX} as a function of T_E for Model III at three different values of SR.

The variation of the irreversibilities (I) as a function of the evaporator temperature for three different values of SR for Model III is illustrated in Figure 12. It can be observed that the I values present an opposite behavior than that observed for the η_{EX} in Figure 11, since a decrease in irreversibilities leads to an exergy efficiency increase. For this system, the I values are almost the same independently of the SR value.

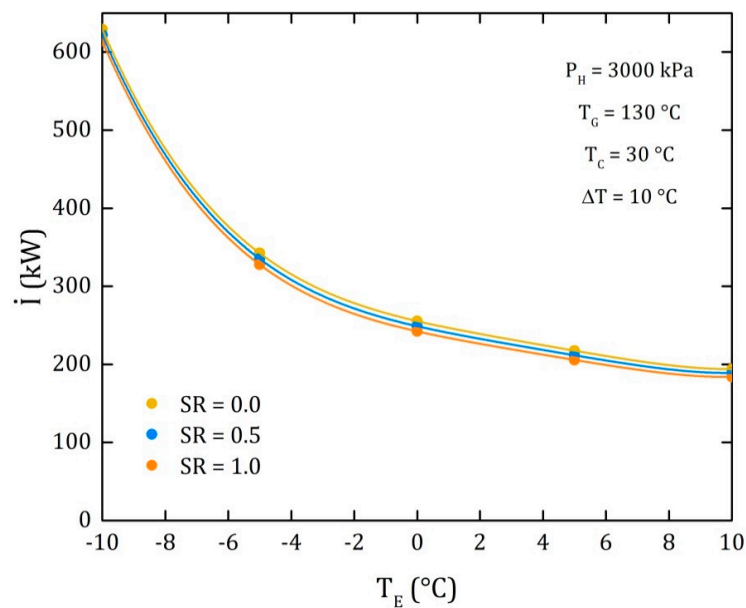


Figure 12. Irreversibilities as a function of T_E for Model III at three different values of SR.

Figure 13 shows the exergy efficiency as a function of turbine efficiency for Model III at three different values of SR. It can be seen that η_{EX} increases with the increment of η_T . This behavior was expected, since by increasing η_T , the turbine produces more work, thus increasing the exergy efficiency of the entire system. In addition, it can be observed that at low values of η_T , the η_{EX} are more dependent on the SR values than at high η_T . This happens, since low values of the SR imply that most of the working fluid is expanding in the turbine and very little is being used for the cooling effect and as the η_T is low, thus the η_{EX} is low too. However, at high SR values, a larger part of the working fluid is being used to produce the cooling effect, thus the efficiency of the turbine has a lower effect on the efficiency of the entire system.

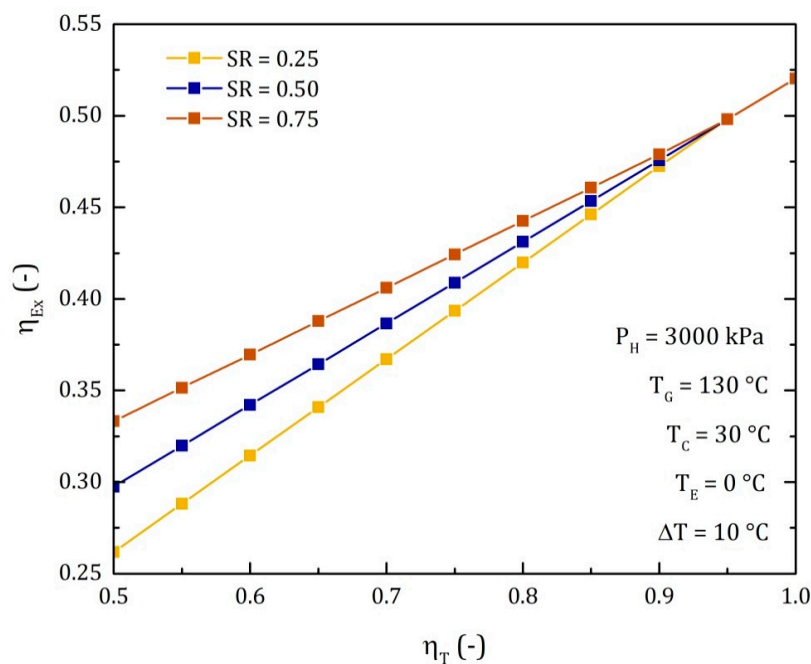


Figure 13. η_{EX} as a function of η_T for Model III at three different values of SR.

Figure 14 illustrates the behavior of η_{EX} as a function of the pressure ratio (PR) at three different values of SR for Model III. As can be observed, the η_{EX} rapidly increases with an increment of SR achieving a maximum value and then decreases. This happens because the increment of PR causes an increase of the work produced by the turbine, and, therefore, η_{EX} , (see Equation (2)). However, if PR continues rising, the pressure difference between P_H and P_L becomes very high, increasing the pump's work, which causes the net power to diminish and, therefore η_{EX} .

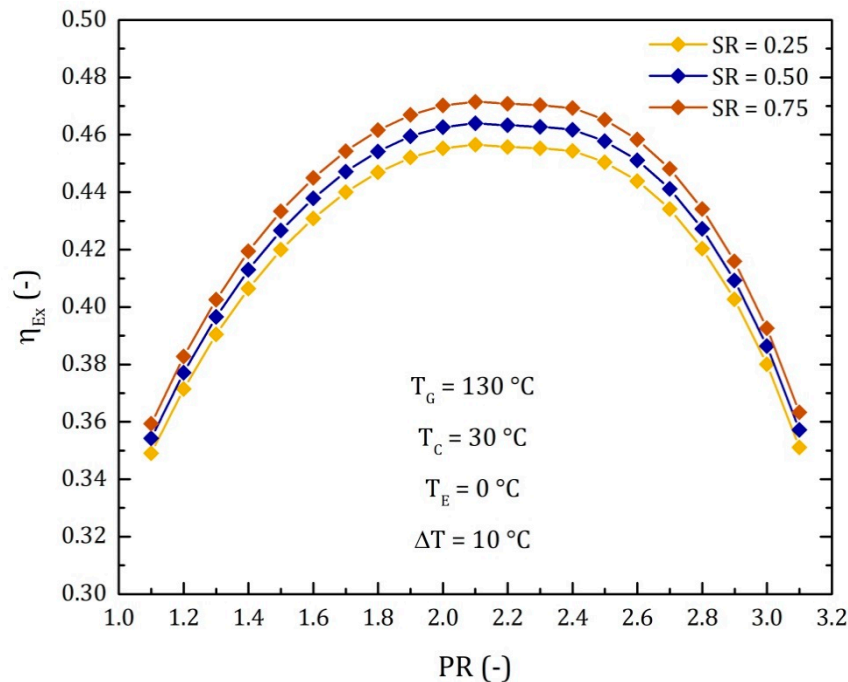


Figure 14. η_{EX} as a function of pressure ratio (PR) for Model III at three different values of SR.

4.3. Comparison of the Performance for the Three Different Thermodynamic Cycles

Figures 15–18 compare the performance of the Goswami cycle (Model I), and the two novel proposed cycles at the same operating conditions.

Figure 15 compares \dot{W}_T and \dot{Q}_E as a function of SR at the conditions of the base case established in Section 4.1. Since in the traditional Goswami cycle, the ammonia mass flow rate is not split at the exit of the rectifier, or into the turbine, thus $SR = 0$. Therefore \dot{W}_T and \dot{Q}_E appear as a single point in Figure 13. As illustrated in Figures 5 and 9, \dot{W}_T decreased, and \dot{Q}_E significantly increased with an increment of SR. It is important to notice that although there is a power decrease in the two proposed models, the decrease of \dot{W}_T is less significant with Model III than with Model II. For an $SR = 0$ the Goswami cycle has the highest $\dot{W}_T = 212$ kW, but just 110 kW of cooling power. For an $SR = 0.5$, \dot{W}_T for Model II is 106 kW, while for Model III is 161 kW and a $\dot{Q}_E = 618$ kW for both cycles. In terms of percentages, \dot{W}_T decreased 50% for Model II and 23% for Model III, and both increased the \dot{Q}_E in about 6 times compared to the Goswami cycle. For $SR = 1$, $\dot{W}_T = 0$ for Model II since all the working fluid produced is used for cooling purposes, while for Model III $\dot{W}_T = 100$ kW, which was around 50% of the power produced by the turbine, compared with the Goswami cycle, but \dot{Q}_E was about 10 times higher than that produced with the Goswami cycle. This considerable increase shows the high capability of Model III to produce a cooling effect and still produce a reasonable amount of electrical power.

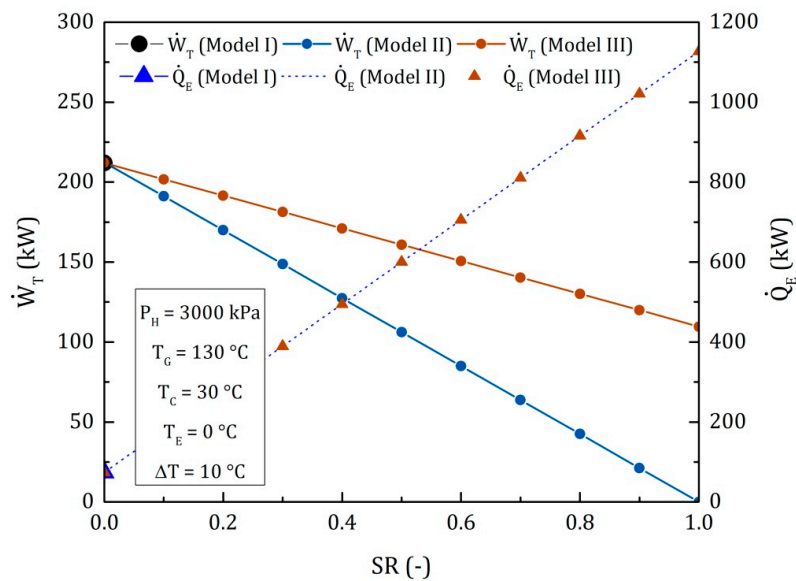


Figure 15. Comparison of \dot{W}_T and \dot{Q}_E as a function of SR for the three models.

Figure 16 compares the EUF as a function of SR for the three models. As can be seen, the EUF values increased with the increment of SR. The minimum value of the EUF for the three models was 0.17, and it was obtained at SR = 0. The maximum EUF values for Models II and III were 0.66 and 0.61, respectively, at SR = 1. As was previously mentioned, this significant increase was due to the considerable increment of \dot{Q}_E .

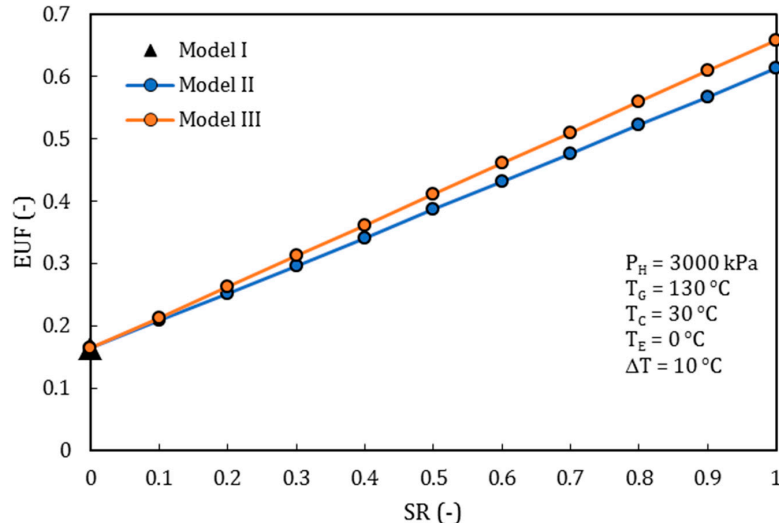


Figure 16. Comparison of the EUF as a function of SR for the three models.

Figure 17 compares the η_{EX} for the three different cycles. As shown, the η_{EX} slightly increased for Model III with the increment of SR, which means that the proposed cycle with a flow extraction in the turbine was better than the conventional Goswami cycle for any SR value. In addition, it can be seen that the η_{EX} significantly decreased with the increment of SR for Model II.

Figure 18 compares the I for the three different cycles. As it can be observed, the I increased for Model II from 251 kW at SR = 0, up to 344 kW at SR = 1. In addition, it is shown that the I decreased for Model III with the increment of SR. The I values for Models II and III were in concordance with the η_{EX} values reported in Figure 17, since an increment in the irreversibilities, led to a decrement in the η_{EX} and vice versa.

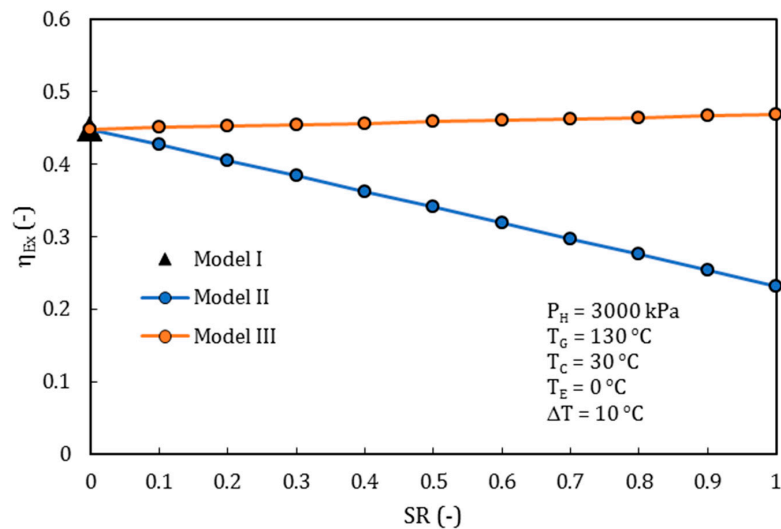


Figure 17. Comparison of the η_{EX} as a function of SR for the three models.

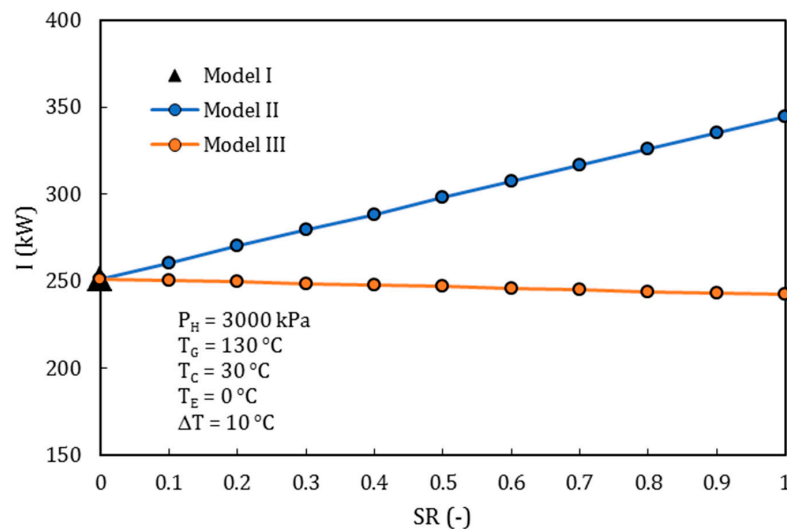


Figure 18. Comparison of the I as a function of SR for the three models.

5. Conclusions

Two novel thermodynamic cycles based on the Goswami cycle were proposed. These cycles have the capability of producing a considerably high amount of cooling power compared to that produced with the Goswami cycle. The three cycles were analyzed based on the first and second laws of thermodynamics.

For Model II, it was shown that the power produced by the turbine decreased, and the cooling power increased considerably with the increment of the split ratio. The increment of the cooling power caused a significant increment in the energy utilization factor, but with an increment of the system irreversibilities, which caused a decrease in the exergy efficiency.

On the other hand, from the analysis of Model III, it was also shown that the power produced by the turbine decreased while the cooling power increased as the split ratio augmented; however, the system irreversibilities decreased significantly with the increment of the split ratio, which allowed an increase of the exergy efficiency.

From the comparison among the three models, it was proven that the Goswami cycle produced the highest amount of electric power; however, the cooling power was considerably much lower than that produced with Model II and Model III. For a split ratio of 0.5, the power produced by the turbine

decreased 50% with Model II, and 23% with Model III, respectively, but the cooling power achieved with the novel cycles was 6 times higher than that produced with the Goswami cycle. For an SR value of 1, it was shown that the power produced by the turbine was zero with Model II, since all the working fluid produced was used for cooling purposes, while for Model III the power was around 100 kW, which was about 50% of the power produced by the turbine, compared with the Goswami cycle, but \dot{Q}_E was about 10 times higher than that produced with the conventional cycle.

Author Contributions: W.R. proposed the original idea and analyzed the results. K.S.-S. proposed the novel thermodynamic cycles, developed the mathematical models for the three cycles, and wrote the results section. J.A.H.-M. and J.C.J.-G. modeled the thermodynamic cycles and wrote part of the paper. A.P. carried out the bibliographic review. All authors have read and agreed to the published version of the manuscript.

Funding: This research received no external funding.

Conflicts of Interest: The authors declare no conflict of interest.

Nomenclature

EBP	Energy balance pump
EBEc	Energy balance economizer
EUf	Energy Utilization Factor (dimensionless)
h	Specific enthalpy (kJ/kg)
I	Irreversibility (kW)
m	Mass flow rate (kg/s)
P	Pressure (kPa)
Q	Heat power (kW)
q	Vapor fraction (dimensionless)
RP	Pressure ratio
SR	Split ratio (dimensionless)
T	Temperature (°C)
W	Mechanical power (kW)
X	Ammonia concentration (% in weight)
Greek letters	
η	Efficiency (dimensionless)
ΔT	Temperature increment (°C)
Subscripts	
A	Absorber
C	Condenser
Cool	Cooler
E	Evaporator
Ec	Economizer
EX	Exergy
G	Generator
H	High
Int	Intermediate
L	Low
Net	Net
P	Pump
R	Reheater
r	Refrigerant
Re	Rectifier
T	Turbine
0	Environment state

Table A1. Cont.

$P_2 = P_3 = P_4 = P_5 = P_7 = P_8 = P_9 = P_{10} = 30 \text{ bar}, P_1 = P_6 = P_{11} = P_{12} = P_{14} = 4.29 \text{ bar}, P_{13} = P_{15} = 11.67 \text{ bar}$											
Property	0	0.1	0.2	0.3	0.4	0.5	0.6	0.7	0.8	0.9	1
T_{13} (°C)	38.59	38.59	38.59	38.59	38.59	38.59	38.59	38.59	38.59	38.59	38.59
X_{13}	0.995	0.995	0.995	0.995	0.995	0.995	0.995	0.995	0.995	0.995	0.995
h_{13} (kJ/kg)	1291	1291	1291	1291	1291	1291	1291	1291	1291	1291	1291
s_{13} (kJ/kg °C)	4.285	4.285	4.285	4.285	4.285	4.285	4.285	4.285	4.285	4.285	4.285
m_{13} (kg/s)	0	0.1	0.2	0.3	0.4	0.5	0.6	0.7	0.8	0.9	1
T_{14} (°C)	30	30	30	30	30	30	30	30	30	30	30
X_{14}	0.995	0.995	0.995	0.995	0.995	0.995	0.995	0.995	0.995	0.995	0.995
h_{14} (kJ/kg)	141.8	141.8	141.8	141.8	141.8	141.8	141.8	141.8	141.8	141.8	141.8
s_{14} (kJ/kg °C)	0.4995	0.4995	0.4995	0.4995	0.4995	0.4995	0.4995	0.4995	0.4995	0.4995	0.4995
m_{14} (kg/s)	0	0.1	0.2	0.3	0.4	0.5	0.6	0.7	0.8	0.9	1
T_{15} (°C)	0.1604	0.1604	0.1604	0.1604	0.1604	0.1604	0.1604	0.1604	0.1604	0.1604	0.1604
X_{15}	0.995	0.995	0.995	0.995	0.995	0.995	0.995	0.995	0.995	0.995	0.995
h_{15} (kJ/kg)	141.8	141.8	141.8	141.8	141.8	141.8	141.8	141.8	141.8	141.8	141.8
s_{15} (kJ/kg °C)	0.5463	0.5463	0.5463	0.5463	0.5463	0.5463	0.5463	0.5463	0.5463	0.5463	0.5463
m_{15} (kg/s)	0	0.1	0.2	0.3	0.4	0.5	0.6	0.7	0.8	0.9	1
\dot{Q}_G (kW)	1806	1806	1806	1806	1806	1806	1806	1806	1806	1806	1806
\dot{Q}_{reca} (kW)	35.85	35.85	35.85	35.85	35.85	35.85	35.85	35.85	35.85	35.85	35.85
\dot{Q}_A (kW)	1633	1633	1633	1633	1633	1633	1633	1633	1633	1633	1633
\dot{Q}_C (kW)	0	114.9	229.9	344.8	459.7	574.7	689.6	804.6	919.5	1034	1149
\dot{Q}_{rect} (kW)	96.12	96.12	96.12	96.12	96.12	96.12	96.12	96.12	96.12	96.12	96.12
\dot{Q}_{SHE} (kW)	1655	1655	1655	1655	1655	1655	1655	1655	1655	1655	1655
\dot{W}_B (kW)	20.21	20.21	20.21	20.21	20.21	20.21	20.21	20.21	20.21	20.21	20.21
\dot{W}_T (kW)	228	216.2	204.4	192.5	180.7	168.9	157	145.2	133.4	121.5	109.7
FUE	0.1646	0.2142	0.2638	0.3133	0.3629	0.4124	0.462	0.5115	0.5611	0.6106	0.6602
E_{fEX}	0.4805	0.4793	0.4782	0.4771	0.476	0.4749	0.4738	0.4726	0.4715	0.4704	0.4693
I (kW)	236.1	236.6	237.1	237.6	238.1	238.6	239.1	239.6	240.1	240.6	241.1

References

1. Kalina, A.I. Combined cycle and waste heat recovery power systems based on a novel thermodynamic energy cycle utilizing low-temperature heat for power generation. In *1983 Joint Power Generation Conference*; Society of Mechanical Engineers: New York, NY, USA, 1983.
2. Kalina, A.I. Combined-Cycle system with novel bottoming cycle. *J. Eng. Gas Turbines Power* **1984**, *106*, 737–742. [[CrossRef](#)]
3. El-Sayed, Y.M.; Tribus, M. Thermodynamic properties of water-ammonia mixtures: Theoretical implementation for use in power cycles analysis. Presented at the Winter Annual Meeting of the American Society of Mechanical Engineers, Miami Beach, FL, USA, 9 December 1985; p. 89.
4. El-Sayed, Y.M.; Tribus, M. A theoretical comparison of the Rankine and Kalina cycles. In *Proceedings of the Analysis of Energy Systems, Design and Operation*, Presented at the Winter Annual Meeting of the American Society of Mechanical Engineers, Miami Beach, FL, USA, 9 December 1985; p. 97.
5. Marston, C.H. Parametric analysis of the Kalina cycle. *J. Eng. Gas Turbines Power* **1990**, *112*, 107–116. [[CrossRef](#)]
6. Park, Y.M.; Sonntag, R.E. A preliminary study of the Kalina power cycle in connection with a combined cycle system. *Int. J. Energy Res.* **1990**, *14*, 153–162. [[CrossRef](#)]
7. Rogdakis, E.D.; Antonopoulos, K.A. A high efficiency $\text{NH}_3/\text{H}_2\text{O}$ absorption power cycle. *Heat Recovery Syst. CHP* **1991**, *11*, 263–275. [[CrossRef](#)]
8. Nag, P.K.; Gupta, A.V. Exergy analysis of the Kalina cycle. *Appl. Therm. Eng.* **1998**, *18*, 427–439. [[CrossRef](#)]
9. Dejfors, C.; Thorin, E.; Svedberg, G. Ammonia-Water power cycles for direct-fired cogeneration applications. *Energy Convers. Manag.* **1998**, *39*, 1675–1681. [[CrossRef](#)]
10. Goswami, D. Solar thermal power technology: Present status and ideas for the future. *Energy Sources* **1998**, *20*, 137–145. [[CrossRef](#)]
11. Xu, F.; Goswami, D.Y.; Bhagwat, S.S. A combined power/cooling cycle. *Energy* **2000**, *25*, 233–246. [[CrossRef](#)]
12. Lu, S.; Goswami, D.Y. Theoretical analysis of ammonia based combined power/refrigeration cycle at low refrigeration temperatures. *Sol. Eng.* **2002**, 117–126. [[CrossRef](#)]
13. Hasan, A.A.; Goswami, D.Y.; Vijayaraghavan, S. First and second law analysis of a new power and refrigeration thermodynamic cycle using a solar heat source. *Sol. Energy* **2002**, *73*, 385–393. [[CrossRef](#)]
14. Hasan, A.A.; Goswami, D.Y. Exergy analysis of a combined power and refrigeration thermodynamic cycle driven by a solar heat source. *J. Sol. Energy Eng.* **2003**, *125*, 55–60. [[CrossRef](#)]
15. Tamm, G.; Goswami, D.Y.; Lu, S.; Hasan, A.A. Theoretical and experimental investigation of an ammonia-water power and refrigeration thermodynamic cycle. *Sol. Energy* **2004**, *76*, 217–228. [[CrossRef](#)]
16. Vijayaraghavan, S.; Goswami, D.Y. Organic working fluids for a combined power and cooling cycle. *J. Energy Resour. Technol.* **2005**, *127*, 125–130. [[CrossRef](#)]
17. Martin, C.; Goswami, D.Y. Effectiveness of cooling production with a combined power and cooling thermodynamic cycle. *Appl. Therm. Eng.* **2006**, *26*, 576–582. [[CrossRef](#)]
18. Vidal, A.; Best, R.; Rivero, R.; Cervantes, J. Analysis of a combined power and refrigeration cycle by the exergy method. *Energy* **2006**, *31*, 3401–3414. [[CrossRef](#)]
19. Zhang, N.; Lior, N. Development of a novel combined absorption cycle for power generation and refrigeration. *J. Energy Resour. Technol.* **2007**, *129*, 254–265. [[CrossRef](#)]
20. Boza, J.J.; Lear, W.E.; Sherif, S.A. Performance of a novel semiclosed gas-turbine refrigeration combined cycle. *J. Energy Resour. Technol.* **2008**, *130*. [[CrossRef](#)]
21. Demirkaya, G.; Vasquez Padilla, R.; Goswami, D.Y.; Stefanakos, E.; Rahman, M.M. Analysis of a combined power and cooling cycle for low-grade heat sources. *Int. J. Energy Res.* **2011**, *35*, 1145–1157. [[CrossRef](#)]
22. Ryu, C.; Tiffany, D.R.; Crittenden, J.F.; Lear, W.E.; Sherif, S.A. Dynamic modeling of a novel cooling, heat, power, and water microturbine combined cycle. *J. Energy Resour. Technol.* **2010**, *132*. [[CrossRef](#)]
23. Padilla, R.V.; Archibold, A.R.; Demirkaya, G.; Besarati, S.; Goswami, D.Y.; Rahman, M.M.; Stefanakos, E.L. Performance analysis of a Rankine cycle integrated with the Goswami combined power and cooling cycle. *J. Energy Resour. Technol.* **2012**, *134*. [[CrossRef](#)]
24. Mendoza, L.C.; Ayou, D.S.; Navarro-Esbri, J.; Bruno, J.C.; Coronas, A. Small capacity absorption systems for cooling and power with a scroll expander and ammonia based working fluids. *Appl. Therm. Eng.* **2014**, *72*, 258–265. [[CrossRef](#)]

25. Ayou, D.S.; Bruno, J.C.; Coronas, A. Combined absorption power and refrigeration cycles using low-and mid-grade heat sources. *Sci. Technol. Built Environ.* **2015**, *21*, 934–943. [[CrossRef](#)]
26. Muye, J.; Ayou, D.S.; Saravanan, R.; Coronas, A. Performance study of a solar absorption power-cooling system. *Appl. Therm. Eng.* **2016**, *97*, 59–67. [[CrossRef](#)]
27. Barkhordarian, O.; Behbahaninia, A.; Bahrampoury, R. A novel ammonia-water combined power and refrigeration cycle with two different cooling temperature levels. *Energy* **2017**, *120*, 816–826. [[CrossRef](#)]
28. Jiang, L.; Lu, H.; Wang, R.; Wang, L.; Gong, L.; Lu, Y.; Roskilly, A.P. Investigation on an innovative cascading cycle for power and refrigeration cogeneration. *Energy Convers. Manag.* **2017**, *145*, 20–29. [[CrossRef](#)]
29. Shankar, R.; Srinivas, T. Performance investigation of Kalina cooling cogeneration cycles. *Int. J. Refrig.* **2018**, *86*, 163–185. [[CrossRef](#)]
30. Shankar, R.; Srinivas, T.; Reddy, V. Investigation of solar cooling cogeneration plant. *Appl. Sol. Energy* **2018**, *54*, 65–70. [[CrossRef](#)]
31. Cengel, Y.A.; Boles, M.A. *Thermodynamics*, 7th ed.; McGraw-Hill: New York, NY, USA, 2011.
32. Ibrahim, O.M.; Klein, S.A. Thermodynamic properties of ammonia-water mixtures. *ASHRAE Trans. Symp.* **1993**, *21*, 1495.



© 2020 by the authors. Licensee MDPI, Basel, Switzerland. This article is an open access article distributed under the terms and conditions of the Creative Commons Attribution (CC BY) license (<http://creativecommons.org/licenses/by/4.0/>).